

The Production of Anti-Matter in our Galaxy

Pascal Chardonnet^{a,b}, Jean Orloff^a and Pierre Salati^{a,b}

*a) Laboratoire de Physique Théorique ENSLAPP, BP110, F-74941
Annecy-le-Vieux Cedex, France.*

b) Université de Savoie, BP1104 73011 Chambéry Cedex, France.

Abstract

The discovery of a single anti-helium nucleus in the cosmic ray flux would definitely point toward the existence of stars and even of entire galaxies made of anti-matter. The presence of anti-nuclei in cosmic rays has actually profound implications on the fundamental question of the baryon asymmetry of the universe. It is therefore crucial to determine the amount of anti-matter which our own galaxy already produces through the spallation of high-energy protons on the interstellar gas of the galactic disk. We have used here a coalescence model to assess the amount of anti-deuterium and anti-helium $^3\bar{\text{He}}$ present in cosmic rays together with anti-protons. The propagation of cosmic rays in the galaxy is described through a two-zone diffusion model which correctly describes the observed abundances. We find that the \bar{D}/p ratio exceeds 10^{-9} above a momentum per anti-nucleon of ~ 4 GeV/c. Would the universe be purely made of matter, the AMS collaboration should be able to detect a few anti-deuterons during the space station stage of the experiment. However, the $^3\bar{\text{He}}/p$ abundance does not exceed $\sim 4 \times 10^{-13}$. Heavier anti-nuclei are even further suppressed.

1 Introduction.

The amount of anti-matter in cosmic rays is about to be measured with unequalled accuracy by the space shuttle borne spectrometer of the AMS collaboration [1]. One of the most exciting goals of the experiment is the possible detection of anti-nuclei in the cosmic radiation. It is generally believed that the observation of a single anti-helium or anti-carbon would undoubtedly signal the presence of stars made of anti-matter. Such a discovery would be of paramount importance as regards the existence of a baryon symmetry in the universe and has therefore strong cosmological implications.

That is why it is crucial to ascertain that cosmic rays do not already contain detectable traces of anti-nuclei which could have been directly manufactured in our galaxy. We know for instance that a fraction $\bar{p}/p \sim 2 \times 10^{-4}$ of anti-protons is produced by the spallation of cosmic ray protons on the interstellar gas of the galactic disk. In this letter, we compute the abundance of anti-deuterium \bar{D} and anti-helium ${}^3\bar{H}e$ produced through the interaction of high-energy protons with the interstellar hydrogen.

That calculation requires two ingredients. First, we need to evaluate the production cross section of anti-nuclei during the interaction of a high-energy proton with a proton at rest. Anti-deuterons are formed by the fusion of an anti-proton and anti-neutron pair. We have used here a factorization scheme together with a coalescence model [2] which we discuss in section 2. Our estimates of the probability for anti-deuterium production are in fairly good agreement with the accelerator data collected at Serpukhov and at the ISR [3, 4, 5]. The anti-helium ${}^3\bar{H}e$ is predominantly formed through the production of anti-tritium \bar{T} which subsequently decays into ${}^3\bar{H}e$. Then, in section 3, we recall the salient features of the two-zone diffusion model that takes care of the propagation of anti-nuclei in the galaxy from the production regions to the earth. Finally, our estimates of the cosmic ray abundances \bar{D}/p and ${}^3\bar{H}e/p$ are discussed in section 4. We find that the \bar{D}/p ratio exceeds 10^{-9} above a momentum per anti-nucleon of ~ 4 GeV/c. Would the universe be purely made of matter, the AMS collaboration should still be able to detect a few anti-deuterons during the space station stage of the experiment. However, the ${}^3\bar{H}e/p$ abundance does not exceed $\sim 4 \times 10^{-13}$. Heavier anti-nuclei are even further suppressed.

2 Factorization and coalescence.

Our goal at this point is to establish the Lorentz-invariant cross section for the production of the anti-nucleus χ during the interaction between two protons. Unless stated otherwise, the subsequent reasoning will be performed in the center of mass frame of the proton-proton collision with total available energy \sqrt{s} and total cross section $\sigma_{\text{p-p}}^{\text{tot}}$. The number $d\mathcal{N}_\chi$ of species χ created during a single interaction and whose momenta are \vec{k}_χ is related to the corresponding differential probability of production by

$$d\mathcal{N}_\chi = \mathcal{F}_\chi(\sqrt{s}, \vec{k}_\chi) d^3 \vec{k}_\chi . \quad (1)$$

This probability \mathcal{F}_χ may be expressed in turn as a function of the Lorentz-invariant differential cross section

$$E_\chi \frac{d^3 \sigma_\chi}{d^3 \vec{k}_\chi}(\sqrt{s}, \vec{k}_\chi) = E_\chi \mathcal{F}_\chi(\sqrt{s}, \vec{k}_\chi) \sigma_{\text{p-p}}^{\text{tot}} , \quad (2)$$

which we want to evaluate. The anti-nucleus energy E_χ cannot exceed the upper bound

$$E_\chi^{\text{max}} = \frac{s - M_X^2 + m_\chi^2}{2\sqrt{s}} , \quad (3)$$

where M_X denotes the minimum mass of the nucleon system (X) that is created with the anti-nucleus. As a result of the conservation of the baryon number, each anti-nucleon is actually forced to be produced together with an additional nucleon. When an anti-proton is created, for instance, three protons remain in the final state and $M_X = 3m_p$. As regards the anti-deuterium production, $M_X \simeq 4m_p$ while it is $5m_p$ for anti-tritium.

The invariant cross section for the production of anti-protons is experimentally well known. It is fairly well fitted by the Tan and Ng's parameterization [6] which we have used throughout this analysis. Assuming that the invariance of isospin holds, the anti-neutron production cross section is equal to its anti-proton counterpart. The calculation of the probability for the formation of an anti-nucleus can now be performed in two steps. We first need to estimate the probability for the creation of a group of anti-nucleons. Then, those anti-nucleons fuse together to yield an anti-nucleus. Let us concentrate on the case of anti-deuterons which requires the formation of both an anti-proton and an anti-neutron. We have assumed that factorization holds

at this stage. This means that the production of two anti-nucleons is proportional to the square of the production of one of them, a hypothesis which is reasonably well established at high energies. However, at lower energies, factorization has to break down, if only to respect the kinematic constraints that thresholds are different. We propose to take this into account by assuming in addition that the center of mass energy available for the production of the second anti-nucleon is reduced by twice the energy carried away by the first anti-nucleon

$$\mathcal{F}_{\bar{p},\bar{n}}(\sqrt{s}, \vec{k}_{\bar{p}}, \vec{k}_{\bar{n}}) = \frac{1}{2} \mathcal{F}_p(\sqrt{s}, \vec{k}_p) \mathcal{F}_{\bar{n}}(\sqrt{s} - 2E_{\bar{p}}, \vec{k}_{\bar{n}}) + (\vec{k}_{\bar{p}} \leftrightarrow \vec{k}_{\bar{n}}) . \quad (4)$$

This probability has the merit of vanishing at the physical threshold. However, it introduces the arbitrary Ansatz that the first pair is produced back to back in the center of mass frame of the proton-proton collision. To test how crucial this assumption really is in the final results, we also give plots for a second possible Ansatz, where the nucleon associated to the first anti-nucleon is produced at rest. This simply amounts to replace $\sqrt{s} - 2E_{\bar{p}}$ by $\sqrt{s} - m_p - E_{\bar{p}}$ in the previous formula. As may be already guessed from figure E2, both Ansaeze give similar results. In the plateau regime where the anti-nuclei abundances are fairly independent of the energy, the relative difference between the two assumptions does not exceed 4%. The probability for the production of the $\bar{p} - \bar{n}$ pair is related to the corresponding cross section by

$$\left(\frac{1}{\sigma_{p-p}^{\text{tot}}} \right) \frac{d^6 \sigma_{\bar{p},\bar{n}}}{d^3 \vec{k}_{\bar{p}} d^3 \vec{k}_{\bar{n}}}(\sqrt{s}, \vec{k}_{\bar{p}}, \vec{k}_{\bar{n}}) = \mathcal{F}_{\bar{p},\bar{n}}(\sqrt{s}, \vec{k}_{\bar{p}}, \vec{k}_{\bar{n}}) . \quad (5)$$

Although \mathcal{F} 's are not Lorentz-invariant, this relation allows to check the Lorentz invariance of the factorization Ansatz (4).

Once the anti-proton and the anti-neutron are formed, they combine together to give an anti-deuteron with probability

$$\mathcal{F}_{\bar{D}}(\sqrt{s}, \vec{k}_{\bar{D}}) d^3 \vec{k}_{\bar{D}} = \int d^3 \vec{k}_{\bar{p}} d^3 \vec{k}_{\bar{n}} \mathcal{C}(\vec{k}_{\bar{p}}, \vec{k}_{\bar{n}}) \mathcal{F}_{\bar{p},\bar{n}}(\sqrt{s}, \vec{k}_{\bar{p}}, \vec{k}_{\bar{n}}) . \quad (6)$$

The summation is performed on those anti-nucleon configurations for which

$$\vec{k}_{\bar{p}} + \vec{k}_{\bar{n}} = \vec{k}_{\bar{D}} . \quad (7)$$

The coalescence function $\mathcal{C}(\vec{k}_{\bar{p}}, \vec{k}_{\bar{n}})$ describes the probability for a $\bar{p} - \bar{n}$ pair to yield by fusion an anti-deuteron. That function depends actually on the

difference $\vec{k}_{\bar{p}} - \vec{k}_{\bar{n}} = 2\vec{\Delta}$ between the anti-nucleon momenta so that relation (6) may be expressed as

$$\mathcal{F}_{\bar{D}}(\sqrt{s}, \vec{k}_{\bar{D}}) = \int d^3\vec{\Delta} \mathcal{C}(\vec{\Delta}) \mathcal{F}_{\bar{p}, \bar{n}} \left(\sqrt{s}, \vec{k}_{\bar{p}} = \frac{\vec{k}_{\bar{D}}}{2} + \vec{\Delta}, \vec{k}_{\bar{n}} = \frac{\vec{k}_{\bar{D}}}{2} - \vec{\Delta} \right) . \quad (8)$$

Notice that the formation of the anti-nucleon pair is implicitly assumed to be independent of the later coalescence process where the anti-nucleons melt together to form the anti-deuteron [2]. This is well justified by the large difference between the binding and pair creation energies. As a matter of fact, an energy of ~ 3.7 GeV is required to form an anti-deuteron whereas the binding energy of the latter is $B \sim 2.2$ MeV. The coalescence function is therefore strongly peaked around $\vec{\Delta} = \vec{0}$ and expression (8) simplifies into

$$\mathcal{F}_{\bar{D}}(\sqrt{s}, \vec{k}_{\bar{D}}) \simeq \left\{ \int d^3\vec{\Delta} \mathcal{C}(\vec{\Delta}) \right\} \mathcal{F}_{\bar{p}, \bar{n}} \left(\sqrt{s}, \vec{k}_{\bar{p}} = \frac{\vec{k}_{\bar{D}}}{2}, \vec{k}_{\bar{n}} = \frac{\vec{k}_{\bar{D}}}{2} \right) , \quad (9)$$

where the probability for the formation of the $\bar{p} - \bar{n}$ pair has been factored out. From the term in brackets, we build a Lorentz-invariant quantity which we evaluate this time in the rest frame of the anti-deuteron

$$\int \frac{E_{\bar{D}}}{E_{\bar{p}} E_{\bar{n}}} d^3\vec{\Delta} \mathcal{C}(\vec{\Delta}) \simeq \left(\frac{m_{\bar{D}}}{m_{\bar{p}} m_{\bar{n}}} \right) \left(\frac{4}{3} \pi P_{\text{coal}}^3 \right) . \quad (10)$$

In that frame, the anti-nucleons merge together if the momentum of the corresponding two-body reduced system is less than some critical value P_{coal} . That coalescence momentum is the only free parameter of our factorization and coalescence model. The invariant cross section for anti-deuterium production in proton-proton collisions may finally be expressed as

$$E_{\bar{D}} \frac{d^3\sigma_{\bar{D}}}{d^3\vec{k}_{\bar{D}}} = \left(\frac{m_{\bar{D}}}{m_{\bar{p}} m_{\bar{n}}} \right) \left(\frac{4}{3} \pi P_{\text{coal}}^3 \right) \times \frac{1}{2\sigma_{p-p}^{\text{tot}}} \left\{ E_{\bar{p}} \frac{d^3\sigma_{\bar{p}}}{d^3\vec{k}_{\bar{p}}} (\sqrt{s}, \vec{k}_{\bar{p}}) E_{\bar{n}} \frac{d^3\sigma_{\bar{n}}}{d^3\vec{k}_{\bar{n}}} (\sqrt{s} - 2E_{\bar{p}}, \vec{k}_{\bar{n}}) + (\vec{k}_{\bar{p}} \leftrightarrow \vec{k}_{\bar{n}}) \right\} , \quad (11)$$

with $\vec{k}_{\bar{p}} = \vec{k}_{\bar{n}} = \vec{k}_{\bar{D}}/2$. The dependence on P_{coal} comes only from the multiplicative P_{coal}^3 prefactor.

Theoretical values for P_{coal} range from $\sqrt{m_p B} \sim 46$ MeV, naively derived from the anti-deuteron binding energy, up to 180 Mev as would follow from

a Hulthen parametrization of the deuterium wave function [7]. We therefore expect P_{coal} to lie somewhere in the range between 50 and 200 MeV. Inside this range, since factorization might also involve an unknown coefficient that could be reabsorbed into P_{coal} , we will rather follow a phenomenological approach. We will determine P_{coal} directly from the known experimental results. These have been summarized in terms of P_{coal} on figure 1. Points 1 and 2 are from an experiment carried out at Serpukhov [5], for a center of mass (CM) energy $\sqrt{s} = 11.5$ GeV, at practically vanishing longitudinal CM momentum p_L and at large transverse momentum with $p_\perp = 1.15$ and 1.5 GeV respectively. Points 3, 4 and 5 have been obtained at the ISR [3], with $\sqrt{s} = 53$ GeV, small p_\perp (0.16, 0.21 and 0.30 GeV) and larger p_L (4.8, 5.7 and 8 GeV). Finally point 6 summarizes about 8 ISR data points [4], at vanishing p_L and with p_\perp ranging from 0.2 to 1 GeV. Given the crudeness of our model and the wide range of kinematic regimes explored experimentally, it is quite comforting that all these data are compatible within 2 standard deviations with our predictions from our single parameter model. Notice in that respect that most of the error bars simply ignore systematic errors. The first five data points are all fitted with a coalescence momentum of order 60 MeV. Because the Serpukhov data correspond to a low center of mass energy, a kinematic regime where anti-deuteron production is astrophysically predominant, we have decided to fix the value of P_{coal} at 58 MeV. Increasing this value to 75 MeV would simply double the production of anti-deuterium.

The anti-helium ${}^3\bar{\text{He}}$ nucleus may be formed directly by the fusion of two anti-protons and an anti-neutron. A second possibility is the synthesis of anti-tritium $\bar{\text{T}}$ which subsequently decays into ${}^3\bar{\text{He}}$ with a half-lifetime of ~ 12.3 years. This second mechanism is dominant. It does not suffer from the electromagnetic suppression due to the Coulomb repulsion between the two anti-protons. We have therefore ignored here the direct ${}^3\bar{\text{He}}$ fusion and have concentrated instead on the production of $\bar{\text{T}}$. The corresponding production cross section may be obtained from the direct generalization of the anti-deuteron calculations. This yields

$$E_{\bar{\text{T}}} \frac{d^3\sigma_{\bar{\text{T}}}}{d^3\vec{k}_{\bar{\text{T}}}} = \left(\frac{m_{\bar{\text{T}}}}{m_{\bar{\text{p}}} m_{\bar{\text{n}}}} \right) \left(\frac{4}{3} \pi P_{\text{coal}}^3 \right)^2 \left(\frac{1}{\sigma_{\text{p-p}}^{\text{tot}}} \right)^2 \times \quad (12)$$

$$\left\{ E_{\bar{\text{p}}} \frac{d^3\sigma_{\bar{\text{p}}}}{d^3\vec{k}_{\bar{\text{p}}}} (\sqrt{s}, \vec{k}_1) E_{\bar{\text{p}}} \frac{d^3\sigma_{\bar{\text{p}}}}{d^3\vec{k}_{\bar{\text{p}}}} (\sqrt{s} - 2E_{\bar{\text{p}}}, \vec{k}_2) E_{\bar{\text{p}}} \frac{d^3\sigma_{\bar{\text{p}}}}{d^3\vec{k}_{\bar{\text{p}}}} (\sqrt{s} - 4E_{\bar{\text{p}}}, \vec{k}_3) \right\} .$$

The momenta \vec{k}_1 , \vec{k}_2 and \vec{k}_3 of the three anti-nucleons are all equal to $\vec{k}_{\bar{\text{T}}}/3$

so that their energy $E_{\bar{p}}$ is also the same. Unfortunately, there are no data available to calibrate the coalescence factor in this case. The best we can do is to use the value $P_{\text{coal}} = 58$ MeV extrapolated from the anti-deuterium data. We have checked that relation (12) does not violate the experimental upper bounds [3].

3 The diffusion of cosmic rays in the galaxy.

Cosmic rays are produced when supernovae shocks accelerate the interstellar material of the galactic plane. These high-energy nuclei propagate in the erratic magnetic fields of the disk where they interact on the gas to create secondary cosmic rays. The amount of secondary light elements such as lithium, beryllium and boron (Li-Be-B) is well explained by the spallation of primary carbon, oxygen and nitrogen nuclei. The latter spend ~ 10 million years (My) in the galactic plane where they cross a column density of ~ 15 g cm $^{-2}$. Quite exciting is the measurement of the isotopic ratio between the unstable ^{10}Be and its stable partner ^9Be . The former nucleus has a half-lifetime of 1.6 My and plays the role of a chronometer. A low value is observed and indicates that cosmic rays spend actually 100 My in the galaxy before escaping in outer space. Particles are confined 90% of the time in extended layers above and beneath the matter ridge where they just diffuse without interacting much with the scarce interstellar medium. Therefore, as regards the propagation of cosmic rays, our galaxy may be reasonably well modelled with two main regions. First, cosmic rays are accelerated within a thin disk with radius $0 \leq r \leq R = 20$ kpc and thickness $|z| \leq h = 100$ pc, where they diffuse and interact on atomic and molecular hydrogen. This gaseous plane is sandwiched by extended domains containing irregular magnetic fields, with same radial extension and $|z| \leq L = 3$ kpc. These thick layers play the role of confinement reservoirs. As a matter of fact, the presence of magnetic fields far above the galactic plane is now firmly established by synchrotron radiation as mentioned by Badwar [8]. On average, the intensity of the magnetic field decreases from ~ 5 μG in the plane down to 1 μG at a height of 5 kpc. Note that magnetic fields have also been detected in other galaxies [9]. Therefore, the transport of high-energy particles crucially depends on their diffusion across the chaotic magnetic fields of the galaxy. We will assume

here an isotropic diffusion with coefficient given by the empirical value

$$K = 6 \times 10^{23} \text{ m}^2 \text{s}^{-1} \left(1 + \frac{\mathcal{R}}{3 \text{ GV}} \right)^{0.6}, \quad (13)$$

where $\mathcal{R} = p/Z$ is the particle rigidity. The diffusion coefficient K is constant at low energies, but increases with the rigidity beyond a critical value of 3 GV.

We follow here the analysis of Webber, Lee and Gupta [10]. The authors showed that the two-zone diffusion model presented above is in good agreement with the observed primary and secondary nuclei abundances. Assuming that steady state holds, the distribution of cosmic ray protons may be derived from the diffusion equation

$$\begin{aligned} \frac{\partial n_p}{\partial t} &= 0 = \\ &= K \left\{ \frac{\partial^2 n_p}{\partial r^2} + \frac{1}{r} \frac{\partial n_p}{\partial r} + \frac{\partial^2 n_p}{\partial z^2} \right\} - 2h \delta(z) \Gamma_p n_p + 2h \delta(z) Q_p(r), \end{aligned} \quad (14)$$

where $n_p(E_p, r, z)$ is the density of protons with energy E_p at location (r, z) . In the right-hand side of relation (14), the first term describes the diffusion of particles. The second term accounts for the destruction of protons by their interactions with the interstellar medium of the galactic plane. That destruction rate is shown to be very small but has not been neglected in what follows. The disk is only 200 pc thick, hence our approximation of an infinite thinness and the term $2h \delta(z)$. The collision rate of protons with the interstellar hydrogen is given by

$$\Gamma_p = \sigma_{p-p}^{\text{tot}} v_p n_H, \quad (15)$$

where $\sigma_{p-p}^{\text{tot}} \sim 44$ mbarns is the total proton-proton interaction cross section, v_p denotes the velocity and $n_H = 1 \text{ cm}^{-3}$ is the average hydrogen density in the thin matter disk. The last term in relation (14) deals with the sources of high-energy protons. It matches the distribution of supernovae remnants and pulsars as measured by Lyne, Manchester and Taylor [11]

$$Q_p(E_p, r) = Q_p^0(E_p) \rho^{0.6} e^{-3\rho}, \quad (16)$$

with $\rho = r/R$. At the edge of the domain where cosmic rays are confined, the particles escape freely and diffusion becomes inefficient. Thus the density

vanishes at the boundaries of the axi-symmetric domain where cosmic rays propagate. This provides the boundary conditions for solving the diffusion equation (14). Following [10], the density n_p is expanded as a series of the Bessel functions of zeroth order $J_0(\zeta_i \rho)$ where ζ_i is the i th zero of J_0 and where $\rho = r/R$. At fixed proton energy E_p and corresponding rigidity \mathcal{R}_p , the density may be expressed as

$$n_p(r, z) = \sum_{i=1}^{\infty} N_{p,i}(z) J_0(\zeta_i \rho) . \quad (17)$$

The diffusion equation (14) may be Bessel transformed, yielding

$$K \left\{ \frac{d^2 N_{p,i}}{dz^2} - \frac{\zeta_i^2}{R^2} N_{p,i} \right\} - 2h \delta(z) \Gamma_p N_{p,i} + \delta(z) q_i = 0 . \quad (18)$$

The coefficients $q_i = 2h Q_i$ are the Bessel transforms of the source distribution $Q_p(r)$ in the galactic plane

$$q_i = \left\{ \frac{Q_p^{\text{tot}}}{\pi R^2} \right\} \left\{ J_1^{-2}(\zeta_i) \right\} \left\{ \int_0^1 Q_p(\rho) J_0(\zeta_i \rho) \rho d\rho \right\} \left\{ \int_0^1 Q_p(\rho) \rho d\rho \right\}^{-1} , \quad (19)$$

where Q_p^{tot} denotes the total production rate of cosmic ray protons with energy E_p in the entire galactic ridge. We have assumed here that the energy spectrum of the sources has the same shape all over the disk. Therefore, the energy dependence of the coefficients q_i may be factorized out in the term $Q_p^{\text{tot}}(E_p)$ and does not depend on i . The functions $N_{p,i}$ are derived from the requirement that they vanish at the boundary $z = L$ and from the relation

$$2K \left. \frac{dN_{p,i}}{dz} \right|_{z=0} = 2h \Gamma_p N_{p,i}(0) - q_i . \quad (20)$$

Integrating equation (18) across the disk and remembering that the $N_{p,i}$'s are odd functions of the height z leads to the last expression. The cosmic ray proton density may finally be expressed as

$$N_{p,i}(z) = \frac{q_i}{A_{p,i}} \mathcal{F}_i(z) . \quad (21)$$

The vertical distribution $\mathcal{F}_i(z)$ is given by

$$\mathcal{F}_i(z) = \frac{\sinh \left\{ \frac{\alpha_i}{2} (L - |z|) \right\}}{\sinh \left\{ \frac{\alpha_i}{2} L \right\}} , \quad (22)$$

where the parameters α_i are equal to $2\zeta_i/R$. The coefficients A_{p_i} stand for

$$A_{p_i} = 2h\Gamma_p + K\alpha_i \coth\left\{\frac{\alpha_i}{2}L\right\} , \quad (23)$$

and depend on the proton energy E_p through the diffusion coefficient $K(\mathcal{R}_p)$ of relation (13) and, in a lesser extent, through the collision rate Γ_p . These coefficients are actually dominated by the diffusion contribution. In the case of cosmic ray protons, spallation does not play an important role in determining their galactic distribution. It affects heavier nuclei for which the interaction cross section on hydrogen is significantly larger.

The density n_χ of the anti-nucleus species χ may be readily inferred from a similar reasoning. It satisfies the diffusion equation

$$K \Delta n_\chi - 2h \delta(z) \Gamma_\chi n_\chi + 2h \delta(z) Q_\chi(r) = 0 . \quad (24)$$

The source term $Q_\chi(r)$ obtains now from the convolution of the proton energy spectrum n_p with the cross section for production of an anti-nucleus χ in a proton-proton interaction

$$Q_\chi(E_\chi, r) = \int_{E_p^{\min}}^{+\infty} \Gamma_p n_p(E_p, r, z=0) \left\{ \frac{d\mathcal{N}_\chi}{dE_\chi}(E_p \rightarrow E_\chi) \right\} dE_p . \quad (25)$$

The energy threshold above which the cosmic ray proton may produce an anti-nucleus χ depends on the atomic number of the latter. For anti-protons, $E_p^{\min} = 7 m_p$ while it is $17 m_p$ for anti-deuterons and $31 m_p$ for anti-tritons. The differential energy distribution $d\mathcal{N}_\chi/dE_\chi$ corresponds to the anti-nucleus χ with energy E_χ that is produced when a proton with energy E_p collides on an hydrogen atom at rest. It is related to the Lorentz-invariant production cross section σ_χ estimated in section 2

$$\sigma_{p-p}^{\text{tot}} \frac{d\mathcal{N}_\chi}{dE_\chi} = \int_0^\pi 2\pi k_\chi \left\{ E_\chi \frac{d^3\sigma_\chi}{d^3\vec{k}_\chi} \right\} d(-\cos\theta) , \quad (26)$$

where σ_χ corresponds to the process $p + p \rightarrow \chi + X$. The momentum \vec{k}_χ of the outgoing species χ makes an angle θ with respect to the direction of the incoming cosmic ray proton. The production term Q_χ may be expanded in terms of its Bessel transforms S_i . This yields the anti-nucleus distribution

$$n_\chi(E_\chi, r, z) = \sum_{i=1}^{\infty} \left(\frac{2h S_i}{B_{\chi i}} \right) \mathcal{F}_i(z) J_0(\zeta_i \rho) , \quad (27)$$

where

$$B_{\chi i}(E_\chi) = 2h\Gamma_\chi + K(\mathcal{R}_\chi)\alpha_i \coth\left\{\frac{\alpha_i}{2}L\right\} . \quad (28)$$

Relation (27) may be simplified because the Bessel transforms $N_{p i}$ of the proton distribution n_p have all the same energy behavior. The latter is contained in the factor $Q_p^{\text{tot}}(E_p)/K(E_p)$ as may be inferred from expression (21). An effective anti-nucleus multiplicity may therefore be defined as

$$\mathcal{N}_\chi^{\text{eff}}(E_\chi) = \int_{E_p^{\text{min}}}^{+\infty} \left\{ \frac{\Phi_p(E_p)}{\Phi_p(E_\chi)} \right\} \left\{ \frac{d\mathcal{N}_\chi}{dE_\chi}(E_p \rightarrow E_\chi) \right\} dE_p . \quad (29)$$

No convolution with the energy spectrum n_p of the cosmic ray protons is needed any more. The differential flux of protons with energy E_p is denoted here by

$$\Phi_p(E_p) = \frac{1}{4\pi} n_p v_p , \quad (30)$$

and is expressed in units of $\text{cm}^{-2} \text{s}^{-1} \text{sr}^{-1} \text{GeV}^{-1}$. In order to derive that flux, we could have naively computed the proton density n_p from the Bessel expansion (17), provided $Q_p^0(E_p)$ is well known. However, as explained above, cosmic ray protons are produced with the same energy spectrum all over the galactic ridge. Their propagation is also dominated by mere diffusion and not spallation on the interstellar gas. Therefore, their energy spectrum does not depend on the position in the galaxy. The energy dependence of n_p may actually be factorized. As a consequence, the flux ratio that appears in the effective multiplicity (29) is constant throughout the galaxy and may be directly derived from measurements performed at earth. We borrowed the proton spectrum from [12]

$$\Phi_p(E_p) \propto \frac{\mathcal{R}_p^{-2.7}}{\sqrt{1 + (1.5 \text{ GV}/\mathcal{R}_p)^2}} . \quad (31)$$

The distribution of the anti-nucleus species χ may finally be expressed as

$$n_\chi(E_\chi, r, z) = \sum_{i=1}^{\infty} \mathcal{F}_i(z) J_0(\zeta_i \rho) \frac{q_i}{A_{p i} B_{\chi i}} 2h \Gamma_p \mathcal{N}_\chi^{\text{eff}} . \quad (32)$$

Note that the anti-nucleus and proton energies are both equal to E_χ in the last formula. The diffusion coefficient K that appears in the quantities $A_{p i}$ and $B_{\chi i}$ is therefore different for the proton and for the anti-nucleus because at fixed energy, the corresponding rigidities are different. Finally, the energy dependence $Q_p^0(E_p)$ in the proton sources q_i disappears in the ratio n_χ/n_p .

4 Discussion and conclusions.

The flux of cosmic ray anti-protons relative to the flux of protons is plotted (solid line) in figure 2 as a function of the momentum of the particles. The curve drops sharply below a few GeV. At higher energies, it exhibits a plateau where the ratio \bar{p}/p reaches a value of $\sim 2 \times 10^{-4}$, in good agreement with the previous calculation by Gaisser and Schaefer [12]. The \bar{D}/p and ${}^3\bar{\text{He}}/p$ cases are also presented on the same plot. The energy behavior is fairly the same as for the anti-protons. However, the magnitude of the effect is significantly suppressed. To fit on the same diagram, the curves have been scaled by a bench-mark factor of 10^4 for anti-deuterium and of 10^8 for anti-helium ${}^3\bar{\text{He}}$. As explained in section 1, the prescription that sets the energy available to the production of any additional anti-nucleon in a proton-proton collision is not clear. Two options are presented here where the nucleon associated to a final anti-nucleon is either produced back to back with its anti-partner (lower curve) or at rest (upper curve). The effect is negligible since the magnitude of the various plateaux is not affected.

We find that the \bar{D}/p ratio exceeds 10^{-9} above a momentum per anti-nucleon of ~ 4 GeV/c. It reaches a maximum of 6×10^{-9} for a momentum of ~ 20 GeV/c. Note that we have only computed the anti-deuterium yield resulting from the spallations of cosmic ray protons on the interstellar hydrogen. Anti-deuterons may alternatively be produced when anti-protons this time interact on the galactic gas. We nevertheless think that this effect is negligible. On the one hand side, the $p\bar{p}$ interaction needs to be quite elastic to allow for the survival of the incoming anti-proton. On the other hand side, if the collision is not inelastic, the additional anti-neutron is not produced. Most of the time, the anti-proton annihilates. The probability that a second anti-nucleon is created with same momentum as the incoming anti-proton is therefore extremely small. In addition, the anti-proton flux is 4 orders of magnitude fainter as for protons.

During the space station borne stage of the experiment, the AMS collaboration should measure a flux of anti-nucleons with a sensitivity reaching a level of $\sim 10^{-9}$ relative to cosmic ray protons. The corresponding energy per nucleon ranges from a GeV up to 20 GeV. We therefore conclude that AMS should detect a few cosmic ray anti-deuterons.

The ${}^3\bar{\text{He}}/p$ abundance does not exceed $\sim 4 \times 10^{-13}$. Even allowing for a generous error of 2 in our estimates, we conclude that the anti-helium nuclei that are manufactured in our galaxy will not be detected by AMS.

Note that we have actually computed the interstellar flux. The results of figure 2 do not include solar modulation. Since the various curves reach their maxima for a momentum per nucleon in excess of 10 GeV, the effect of solar modulation will just be a slight shift of a fraction of a GeV towards low energies, depending on the specific epoch of the solar cycle. The same conclusions still hold.

As shown in section 1, factorization comes into play for the production of several anti-nucleons during the same proton-proton event. The general trend is a reduction of the yield by a factor larger than 10^4 when the atomic number of the anti-nucleus is increased by one unit. As an illustration, it is clear from figure 2 that the \bar{D}/\bar{p} ratio is $\sim 3 \times 10^{-5}$ while ${}^3\bar{\text{He}}/\bar{D} \sim 7 \times 10^{-5}$. The anti-nuclei with atomic number $A \geq 3$ that are produced through cosmic ray spallations in our galaxy are not detectable by AMS. Alternatively, if anti-matter is processed in anti-stars, the abundance of its various components should be quite similar to the conventional stellar yields. It would follow therefore the same relative proportions as in our own interstellar material. In any case, the detection of a single anti-helium or anti-carbon by the AMS collaboration would be a smoking gun for the presence of large amounts of anti-matter in the universe and for the existence of anti-stars and of anti-galaxies.

Acknowledgements

We would like to express our gratitude toward G. Girardi and G. Mignola for stimulating discussions. This work has been carried out under the auspices of the Human Capital and Mobility Programme of the European Economic Community, under contract number CHRX-CT93-0120 (DG 12 COMA). We also acknowledge the financial support of a Collaborative Research Grant from NATO under contract CRG 930695.

References

- [1] S. Ahlen *et al.*, An Antimatter Spectrometer in Space, *Nucl. Instrum. Meth.*, A350:351, 1994.
- [2] S. T. Butler and C. A. Pearson, Deuterons from High-Energy Proton Bombardment of Matter, *Phys. Rev.*, 129(2):836–842, 1963.
- [3] M. G. Albrow *et al.*, Search for Stable Particles of Charge ≥ 1 and Mass \geq Deuteron Mass, *Nucl. Phys.*, B97:189–200, 1975.
- [4] W. M. Gibson *et al.*, Production of Deuterons and Anti-deuterons in Proton-proton Collisions at the Cern ISR, *Lett. Nuovo Cim.*, 21(6):189–194, 1978.
- [5] V. V. Abramov *et al.*, Production of Deuterons and Anti-deuterons with Large p_\perp in pp and pA Collisions at 70 GeV, *Sov. J. Nucl. Phys.*, 45(5):845–851, 1987.
- [6] L. C. Tan and L. K. Ng, Parametrization of \bar{p} Invariant Cross Section in $p - p$ Collisions Using a New Scaling Variable, *Phys. Rev.*, D26(5):1179–1182, 1982.
- [7] M. A. Braun and V. V. Vechernin, Fragmentation Deuterons From Nucleon Pairing, *Sov. J. Nucl. Phys.*, 36(3):357–362, 1982.
- [8] G. D. Badwar and S. A. Stephens, Hydrostatic Equilibrium of Gas, Extent of Cosmic Ray Confinement, and Radio Emission in the Galaxy, *Ap.J.*, 212:494–506, 1977.
- [9] Y. Sofue, M. Fujimoto and R. Wielebinski, *ARA&A*, 24:459, 1986.
- [10] W. R. Webber, M. A. Lee and M. Gupta, Propagation of Cosmic-ray Nuclei in a Diffusing Galaxy with Convective Halo and Thin Matter Disk, *Ap.J.*, 390:96–104, 1992.
- [11] A. G. Lyne, R. N. Manchester and J. H. Taylor, *MNRAS*, 213:613, 1985.
- [12] T. K. Gaisser and R. K. Schaefer, Cosmic-ray Secondary Antiprotons : a Closer Look, *Ap.J.*, 394:174–183, 1992.

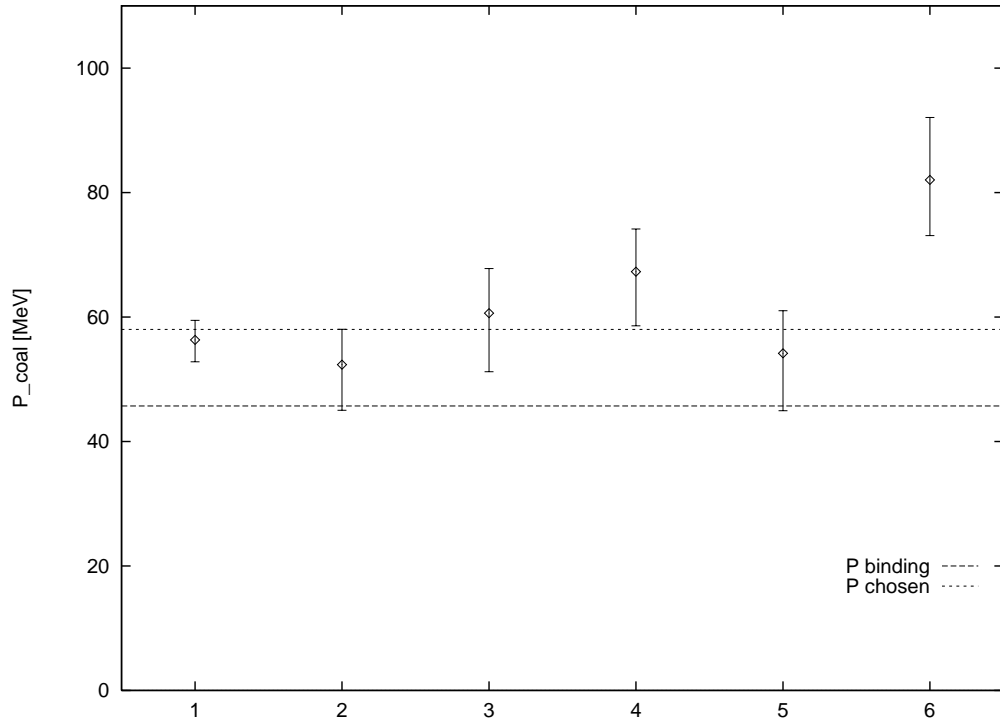


Figure 1: This figure displays various experimental constraints on the coalescence momentum P_{coal} , the only free parameter of the model discussed in section (2). Points 1 and 2 are from Serpukhov with $\sqrt{s} = 11.5$ GeV while all the other data have been collected at the ISR at $\sqrt{s} = 53$ GeV. A coalescence momentum P_{coal} of order 60 MeV provides a reasonable fit of all the points but the last one.

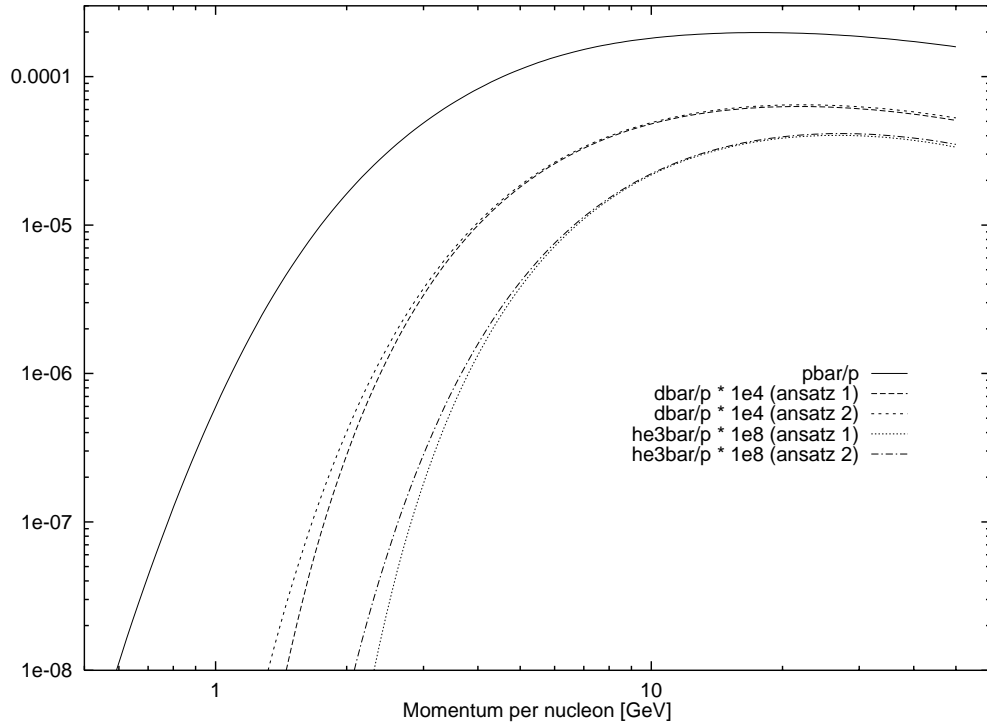


Figure 2: The fluxes of cosmic ray anti-protons and of anti-deuterium and anti-tritium nuclei, relative to the proton flux, are presented as a function of the momentum per nucleon. To fit on the same diagram, the curves have been scaled by a factor of 10^4 for anti-deuterium and of 10^8 for anti-helium ^3He . The doubling of curves corresponds to different factorization schemes as explained in section 1.